International Journal of the Physical Sciences Vol. 5(7), pp. 978-983, July 2010
Available online at http://www.academicjournals.org/IJPS
ISSN 1992 - 1950 ©2010 Academic Journals

Full Length Research Paper

Theoretical investigations for electronic structures and photodissociation of bromine molecule

A. Abdel-Hafiez*, Rageh Atteya and M. E. Medhat

Department of Experimental Nuclear Physics, Nuclear Research Center Atomic Energy Authority, P. O. Box 13759, Cairo, Egypt.

Accepted 31 December, 2009

We have theoretically studied the nonadiabatic transitions among the lower states with $\Omega = 1_u$ symmetry {1_u (Lindeman and Wiesenfeld, 1979) to 1_u (Alexander et al., 2000)} in the photodissociation of Br_2 using the complete active space self-consistent field (CASSCF) computations and the time-independent Schrodinger equations. The CASSCF wave function is formed from a complete distribution of a number of active electrons in a set of active orbitals, which in general constitute a subset of the total occupied space. From the configuration analysis of the CASSCF wave functions, we found that the nonadiabatic transition between 1_u (Bracker et al., 1999) and 1_u (Lindeman and Wiesenfeld, 1979) is a noncrossing type, while that between 1_u (Bracker et al., 1999) and $B^3\Pi_{0+u}$ is a crossing type. The spectroscopic constants for the $X^1\Sigma_g^+$, $A^3\Pi_{1u}$ and $B^3\Pi_{0+u}$ states of Br_2 have been calculated. The absorption cross-section for the ground and the lower excited states in the photodissociation of Br_2 molecule has been presented as well as the numerical estimates of nonadiabatic transition probabilities. Also, the five highest occupied and the five lowest unoccupied orbitals of Br_2 have been calculated.

Key words: Nonadiabatic transitions, broimine molecule, photodissociation.

INTRODUCTION

Classical investigations of the discrete absorption spectrum of halogen molecules, especially Br_2 and I_2, have resulted in the accurate identification of transitions between specific vibrational and rotational levels of these diatomics (Lindeman and Wiesenfeld, 1979). Such analyses have permitted the precise characterization of the potential curves for the bound $X^1\Sigma_g^+$ ground and $B^3\Pi_{0+u}$ excited states. A drawback, common to the above methods, is that such techniques cannot, however, be used for the study of repulsive states or those portions of bound excited states which lie above the thermochemical threshold for dissociation into open-shell atomic fragments in ground configuration with which they correlate.

Diatomic halogen and interhalogen molecules continue to serve as benchmark systems to study photo-dissociation dynamics. Recent experimental activity has been devoted to the study of the orientation and alignment, namely the m_j distributions, of the product angular momentum. Details of the nonadiabatic transition probabilities have been estimated from such analysis for Cl_2 (Bracker et al., 1999; Alexander et al., 2000; Rakitzis and Kitsopoulos, 2002; Bass et al., 2003) and Br_2 (Rakitzis and Kitsopoulos, 2002). Also, recent advances in both experimental and theoretical studies of molecular photodissociation enable us to investigate quite detailed information on the dissociation dynamics.

Asano and Yabushita (2003), calculated the potential curves of I_2 by the spin-orbit configuration interaction (SOCI) method and evaluated the radial derivative coupling elements among the five lower states with $\Omega = 1_u$ symmetry {1_u (Lindeman and Wiesenfeld, 1979) to 1_u (Alexander et al., 2000)} to examine the nonadiabatic transition processes and to compare the results with those of Cl_2 and Br_2. Also, Asano and Yabushita (2003) evaluated the nonadiabatic transition probabilities of Cl_2 and Br_2 by solving the semi classical time-dependent coupled SchrÖdinger equations.

Balasubramanian et al. (1989) calculated the spectroscopic properties and potential curves of I_2 by the complete active space SCF method followed by the

*Corresponding author. E-mail: abdel_hafiez@yahoo.com.

nonrelativistic first-order and second-order configuration interaction (CI) and recent relativistic many-body perturbation methods. Teichteil and Pelissier (1994) calculated the potential curves of I_2 with an *ab initio* relativistic atomic pseudo- potential method and analyzed the available experimental data. Nieuwpoort et al. (1997) employed an all-electron Dirac-Fock method followed by the CCSD (T) calculations. However, none of the previous workers has studied the nonadiabatic transitions in the photodissociation of I_2.

The ability to accurately describe complicated molecular wave functions with only few terms has often been claimed to be one of the major advantages of the MCSCF method (Siegbahn et al., 1981). This simple picture is usually contrasted to the very long expansions encountered in conventional CI methods where the orbitals are not variationally optimized. In the CASSCF method, the philosophy is quite different from that of traditional MCSCF methods, in that it should involve complete sets of multiconfigurational wave functions although, it tends to be rather time consuming, thus providing an ideal path for the systematic study of electron correlation effects in excitation processes involve not only one photon.

A potential energy surface is a mathematical relationship linking molecular structure and the resultant energy. For a diatomic molecule, it is a two-dimensional plot with the internuclear separation on the X - axis and the energy at that bond distance on the Y - axis, producing a curve. For larger systems, the surface has as many dimensions as there are degrees of freedom within the molecule.

Potential energy surfaces may be determined by *ab initio* electronic structure calculations. In this method one performs a large number of electronic structure calculations (which may be very expensive) and then fits the results using a least square procedure. The reliability of the PES depends on the basis set completeness and how well electron correlation is accounted for.

In the paper (Siegbahn et al., 1981), the CASSCF method was presented in detail. In this study, we introduce the brief discussion of the method and presents some experience from an application to the bromine molecule, we calculated the ground and some excited states of Br_2 by the Complete Active Space Self-Consistent Field (CASSCF) computations at 6-31+G(d. p) level and the semi classical time-dependent coupled SchrÖdinger equations.

COMPUTATIONAL METHODS AND THEORY

The CASSCF program used is a part of the GAUSSIAN 03 (Frisch et al., 2003) suite of programs. A CASSCF calculation is a combination of SCF computation with a full configuration interaction calculation involving a subset of the orbitals. The orbitals involved in the CI are known as the active space. In this way, the CASSCF method optimizes the orbitals appropriately for the excited state.

All calculations have been performed using the implementation of the CASSCF procedure and the standard 6-31+G (d. p) basis set available in the Gaussian 03 Frisch et al., 2003). Locations of excited-state minima and transition structures have been carried out by using the methods available in the same program package.

The numerical estimates of nonadiabatic transition probabilities are calculated by using the program of Asano and Yabushita (2003). That program depends on the semi classical theory, in which the total wave function, ψ_e(R (t), r) satisfies the following time-dependent Schrodinger equation

$$i\hbar\partial\Psi_e(R(t),r)/\partial t = [H_e(R(t),r)]\Psi_e(R(t),r)$$

Where H_e is the electronic Hamiltonian, r is the electronic co-ordinate and R (t) is the internuclear distance and the molecular rotation is not considered here. If ψ_e is expand in terms of the adiabatic wave functions, 1_u (Lindeman and Wiesenfeld, 1979) through 1_u (Bass et al., 2003), the expansion coefficients C_n (t) satisfy a set of the first-order coupled equations,

$$i\hbar\ dC_k(t)/dt = \sum_n [E_k\delta_{kn} - i\hbar\upsilon g_{kn}]C_n(t)$$

Where E_k are the eigenvalues of H_e, υ is the relative nuclear velocity, $g_{kn} = \langle 1_u^{(k)} | d/dR | 1_u^{(n)} \rangle$ are the radial derivative (nonadiabatic) coupling elements between $1_u^{(k)}$ and $1_u^{(n)}$ and $|C_n(t)|^2$ stands for the probability of finding the system in the adiabatic state $1_u^{(n)}$. The relative nuclear motion is described by the classical equation of motions.

$$\mu\ d^2R(t)/dt^2 = -\partial E_i/\partial R\ ,$$

Where μ is the reduced mass and E_i is the adiabatic potential energy on which the photodissociation takes place.

RESULTS AND DISCUSSION

The calculated adiabatic potential curves of Br_2 are shown in Figure 1. Spectroscopic constants of the $X^1\Sigma_g^+$, $A^3\Pi_{1u}$ and $B^3\Pi_{0+u}$ states of Br_2 are shown in Table 1 and are in reasonable agreement with the experimental results (Huber and Herzberg, 1979; Coxon, 1973). We thus expect that quantitative results can be obtained for the photodissociation processes with these *ab initio* potential energy curves.

Our calculations for these characteristics have been explored by performing a potential energy surface scan on the model chemistry CASSCF/aug-cc-pVTZ level, where the notation (10,8) defines the complete active space: 10 electrons distributed over 8 molecular orbitals (MOS) {$\sigma_{Br\text{-}Br}^*$, π_x(Br), π_x^*(Br), π_y(Br), π_y^*(Br), $2n_{Br}$, $\sigma_{Br\text{-}Br}$}. The calculated potential curves of Br_2 are shown in Figure 1. Note that the $A^3\Pi_{1u}$ (1_u) and $^1\Pi_u$ (1_u) states correlate to the ground state Br+Br limit, whereas the $B^3\Pi_{0+u}$ (0_u^+) state correlates to the Br+Br* limit. The potential energy curve for another repulsive 1_u state, correlating to the Br+Br* limit, what it means is that potential is implicated in the proposed explanation for the non-limiting β values observed for the Br+Br* product recoil velocity distributions (Cooper et al., 1998). In the numerical calculation of the absorption cross-section

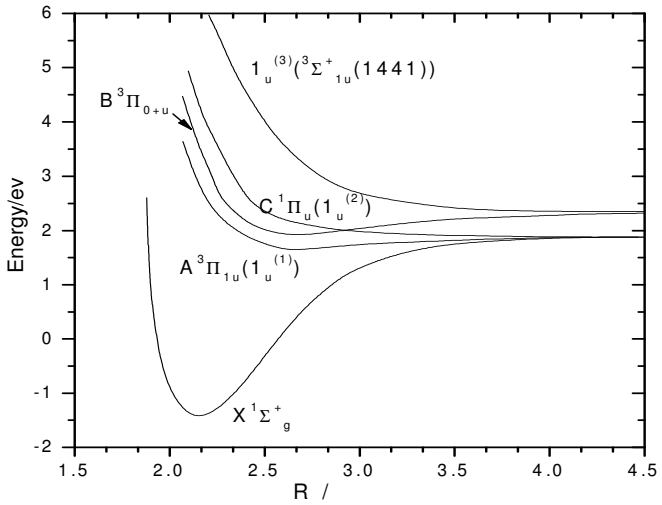

Figure 1. Potential energy curves for ground state Br_2 and for the three excited states determined by CASSCF calculations.

Table 1. Our calculations in comparison with experimental spectroscopic constants (Huber and Herzberg, 1979; Coxon, 1973) for the $X^1\Sigma_g^+$, $A^3\Pi_{1u}$ and $B^3\Pi_{0+u}$ states of Br_2.

		R_e(Å)	D_e(kJ/mol)	ω_e(cm^{-1})	$\omega_e\xi_e$(cm^{-1})
$X^1\Sigma_g^+$	This work	2.304	188.53	320.7	1.24
	Experiment	2.280	190.17	325.3	1.08
$A^3\Pi_{1u}$	This work	2.758	22.57	144.8	2.85
	Experiment	2.690	24.77	153	2.7
$B^3\Pi_{0+u}$	This work	2.760	43.51	163.1	1.91
	Experiment	2.677	44.96	167.6	1.64

R_e, D_e, ω_e and $\omega_e\xi_e$ are the equilibrium bond length, the dissociation energy at equilibrium R for the corresponding state, vibrational frequency characterize, and the anharmonic spectroscopic constants, respectively.

the photodissociation of Br_2 molecule, we used the program by Balint-Kurti et al. (1993) employing the time-dependent quantum dynamical method. The mechanism is assumed to involve the absorption of a photon of ultraviolet radiation which causes an electronic transition in the molecule from a bound to a repulsive electronic state. The two atoms then fly apart under the influence of the forces on the repulsive electronic state causing the molecule to break up into its atomic fragments. This program permits the calculation of cross-sections for molecules in different initial vibrational states.

Our programmed calculations of the total absorption cross section to the A, B and C states are shown in Figure 2a, also portrayed are the partial absorption coefficients from these discrete state, which corresponding to the schematic deconvolution of the total absorption spectrum and indicate that the A - X and particularly, B - X transitions contribute to the continuous absorption at shorter wavelengths(λ < 510 nm); the latter is deemed responsible for the inflexion in the absorption profile at $\lambda \approx$ 460 nm. Electronic absorption spectrum of Br_2 recorded over the wavelength range 300 - 600 nm (solid lone), together with an illustrative decomposition into contributions associated with excitations to the $A^3\Pi_{1u}$ (1u), B3Π0+u (0u+) and 1Πu (1u) states (dot lines).

It also apparent that the first absorption band has a peak at 421.4 nm due to the excitation to the $C^1\Pi_u$ (1_u, Bracker et al., 1999) state and agrees well with both ref (Bass et al., 2003) in which it has a peak at 419.6 nm and the experimental value of 420 nm (Cooper et al., 1998; Balint-Kurti et al., 1993). The calculated absorption cross section to the $^3\Sigma^+_{1u}(1441)$ state in Figure 2b has a maximum at 235.3 nm, which is in reasonable agreement

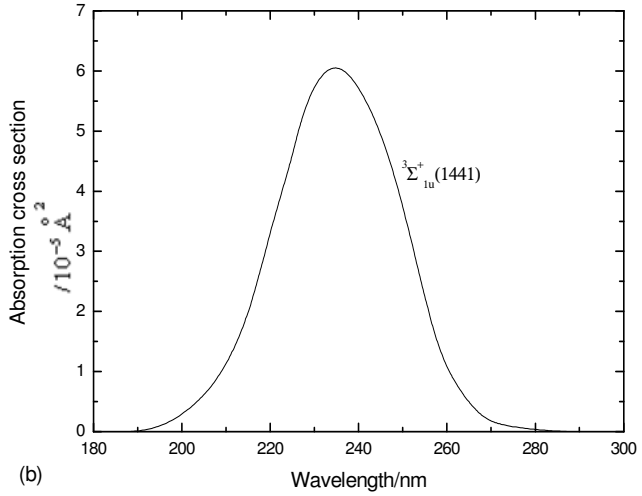

Figure 2b. Absorption cross section to the $^3\Sigma^+_{1u}(1441)$ state of Br_2.

with both of (Asano and Yabushita, 2003) in which it has a peak at 234.8 nm and with the experiment, supporting the tentive assignment (Hubinger and Nee, 1995).

Figure 3a Shows the probabilities after the photoexcitation to the $C^1\Pi_u$ {1_u (Bracker et al., 1999)} state at 355 nm for Br_2 and the nonadiabatic transition from 1_u (Bracker et al., 1999) takes place only to 1_u (Lindeman and Wiesenfeld, 1979). Figure 3b shows the probabilities after the vertical excitation to the $^3\Sigma^+_{1u}(1441)$ 1_u (Alexander et al., 2000) state and the nonadiabatic transition takes place only to 1_u (Rakitzis and Kitsopoulos, 2002).

Table 2 summarizes the low-lying excitations of the parent Br_2 molecule. According to the TD-DFT computations, in both states, the transition σ_z (Br)→ π_z^*(Br-Br) calculated at 8.6373 eV (143.54 nm) and n_x (Br)→ π_z^*(Br-Br), n_y (Br)→ π_z^*(Br-Br) calculated at 2.6446 eV (468.81 nm) are found to dominate the absorption from the estimated oscillator strength f = 0.8774 and f = 0.0004 respectively. Because the excitation energies to the σ_z (Br)→ π_z^*(Br-Br) transition lies very close to the Rydberg transition, the measured spectrum band can be ascribed mainly to the transitions n_x (Br)→ π_z^*(Br-Br) and n_y (Br)→ π_z^*(Br-Br). This indicates that experimental absorption profile will show a maximum cross-section nearby the wavelength of 460 nm.

In order to help better explore the photodissociation channels correlate to the low lying excited states of Br2, we have examined the relevant molecular orbitals. Figure 4 shows the five highest occupied and the five lowest unoccupied orbitals calculated at the TD-DFT/6-311++G (3df, 2pd) level of theory.

The five highest occupied orbitals 31 - 33 correspond to the lone-pair of nonbonding p electrons of the bromine

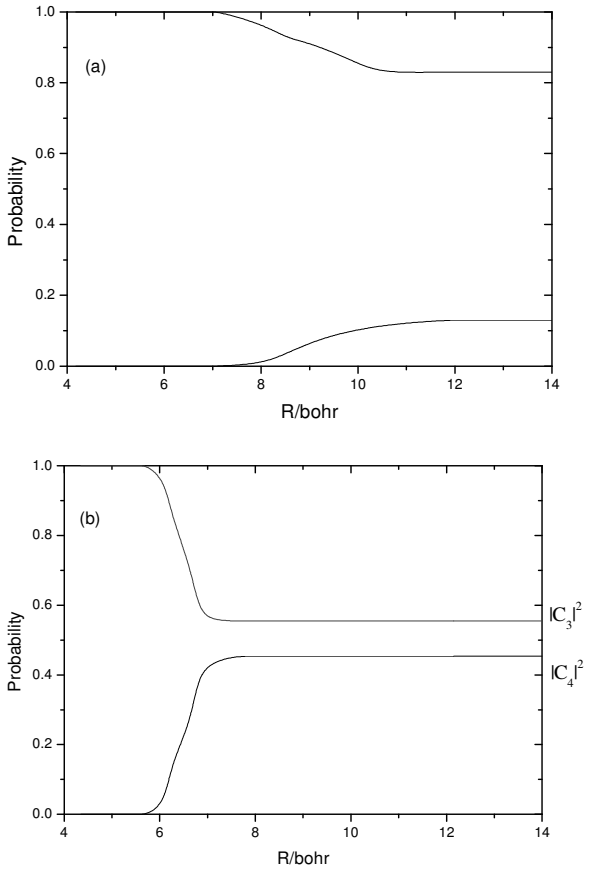

Figure 3. Semi classical probabilities as a function of R with 355 nm photon of Br_2 from the initial excitation to the 1_u (Bracker et al., 1999) ($C^1\Pi_u$) state (Figure 3a) and from the initial excitation to the 1_u (Alexander et al., 2000) ($^3\Sigma^+_{1u}(1441)$) state (Figure 3b).

atoms and 34 - 35 correspond to the bonding p electrons of the bromine atoms. The five lowest unoccupied orbitals 36, 39 and 40 correspond to the excited nonbonding p electrons of the bromine atoms, but 39 and 40 are of higher order, the unoccupied orbitals 37 and 38 can be described as the $\sigma^*_{Br\text{-}Br}$.

Conclusion

We calculated the ground and low-lying excited states of Br_2 by using the Comlete Active Space Self-Consistent Field (CASSCF) computations and examined the spectroscopic constants of the $X^1\Sigma_g^+$, $A^3\Pi_{1u}$ and $B^3\Pi_{0+u}$ states which are found in reasonable agreement with experimental results. Numerical calculations of the absorption cross-section to the A, B and C states for the photodissociation of Br_2 molecule, have been done employing the time-dependent quantum dynamical approach and agree well with experimental results. The

Table 2. TD-DFT calculated excitation energies ΔE (in eV), corresponding main excitations and oscillator strengths f, for the Br_2 molecule in the equilibrium geometry.

Br_2	Main excitation	Transition energies ΔE (eV)	Excitation wavelength/ nm	oscillator strengths
		State		
$^1\Pi_x$	$n_x(Br) \rightarrow \pi_z^*(Br\text{-}Br)$	2.6446	468.81	f = 0.0004
$^1\Pi_y$	$n_y(Br) \rightarrow \pi_z^*(Br\text{-}Br)$	2.6446	468.81	f = 0.0004
$^1\Sigma^-$	$\sigma_y(Br) \rightarrow \pi_z^*(Br\text{-}Br)$	4.6611	266.00	f = 0.0000
$^1\Sigma^+$	$\sigma_x(Br) \rightarrow \pi_z^*(Br\text{-}Br)$	4.6611	266.00	f = 0.0000
$^1\Delta$	$\sigma_z(Br) \rightarrow \pi_z^*(Br\text{-}Br)$	8.6373	143.54	f = 0.8774
$^3\Pi_x$	$n_x(Br) \rightarrow \pi_z^*(Br\text{-}Br)$	1.8508	669.90	f = 0.0000
$^3\Pi_y$	$n_y(Br) \rightarrow \pi_z^*(Br\text{-}Br)$	1.8508	669.90	f = 0.0000
$^3\Sigma^-$	$\sigma_y(Br) \rightarrow \pi_z^*(Br\text{-}Br)$	3.9168	316.55	f = 0.0000
$^3\Sigma^+$	$\sigma_x(Br) \rightarrow \pi_z^*(Br\text{-}Br)$	3.9168	316.55	f = 0.0000
$^3\Delta$	$\sigma_z(Br) \rightarrow \pi_z^*(Br\text{-}Br)$	5.1270	241.83	f = 0.0000

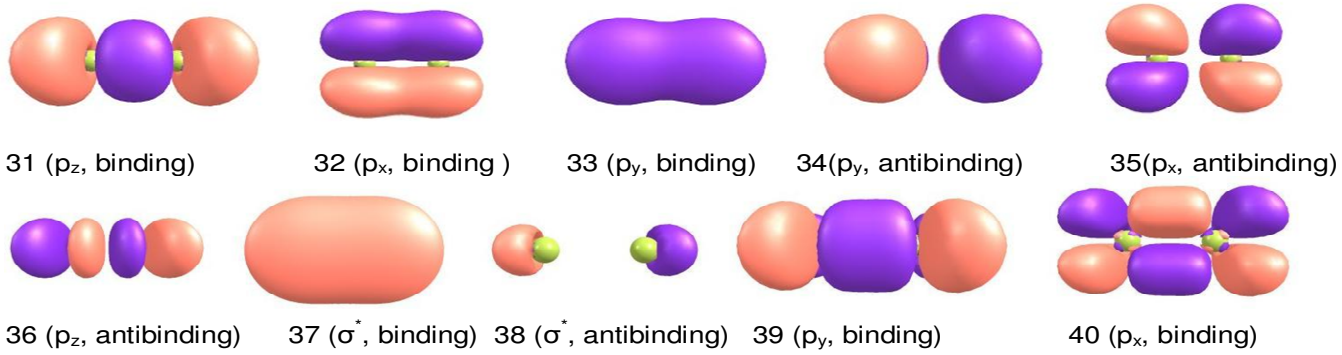

Figure 4. The five highest occupied and the five lowest unoccupied orbitals of Br2 at TD//B3LYP/6-311++G (3df, 2pd) level of theory.

nonadiabatic transition probabilities have been also evaluated in the frame of the semi classical theory.

The five highest occupied and the five lowest unoccupied orbitals of Br_2 could be obtained to explore the photodissociation channels at TD//B3LYP/6-311++G (3df, 2pd) level of theory. Finally, we can say that CASSCF is quite good method to investigate structures on the electronic excited states and photodissociation of bromine molecule and also, produce results of high accuracy.

ACKNOWLEDGMENT

Many thanks to H. Studzinski, Institute for Physical Chemistry, University of Kiel, Germany for his comments and fruitful discusions.

REFERENCES

Alexander AJ, Kim ZH, Kandel SA, Zare RN, Rakitzis TP, Asano Y, Yabushita S (2000). Oriented chlorine atoms as a probe of the nonadiabatic photodissociation dynamics of molecular chlorine, J. Chem. Phys., 113: 9022.

Asano Y, Yabushita SB (2003). Rotational State Distributions of I2(B) from Vibrational Predissociation of I2(B)-Ne, Korean Chem. Soc., 6: 24-703.

Balint-Kurti GG, Mort SP, Marston CC (1993). A computer program to calculate the total energy absorption cross-section for the photodissociation of a diatomic molecule arising from a bound state → repulsive state transition using time dependent quantum dynamical methods, Comput. Phys. Commun., 74: 289.

Bass MJ, Brouard M, Clark AP, Vallance C, Martinez H (2003). Angular momentum alignment of Cl(2P3/2) in the 308 nm photolysis of Cl2 determined using Fourier moment velocity-map imaging, B. Phys. Chem. Chem. Phys., 5: 856.

Bracker AS, Wouters ER, Suits AG, Vasyutinskii OS (1999). Imaging the alignment angular distribution: State symmetries, coherence, and nonadiabatic dynamics in photodissociation, J. Chem. Phys., 110: 6749.

Cooper MJ, Wrede E, Orr-Ewing AJ, Ashfold MNR (1998). Ion imaging studies of the Br(2PJ) atomic products resulting from Br2 photolysis in the wavelength range 260–580 nm, J. Chem. Soc. Faraday Trans. 94: 2901.

Coxon JA, Barrow RF, Long DA, Millen DJ (1973). In Low-lying Electronic States of Diatomic Halogen Molecules Eds. Molecular Spectroscopy. The Chemical Society: London. 1: 177.

Frisch MJ, Trucks GW, Schlegel HB, Scuseria GE, Robb MA (2003). Complete Active Space SCF (CASSCF) and Gaussian 03, Revision B.01, Gaussian Inc., Pittsburgh PA .

Huber K, Herzberg PG (1979). Constants of Diatomic Molecules: Van

Nostrand Reinhold: New York.
Hubinger S, Nee JB (1995). Absorption spectra of Cl2, Br2 and BrCl between 190 and 600 nm, J. Photochem. Photobiol. A: Chem., 1(2): 131.
Li J, Balasubramanian K (1989). Spectroscopic properties and potential energy curves of I2 and I2+, J. Mol. Spectrosc., 138: 162.
Lindeman TG, Wiesenfeld JR (1979). Photodisosiation of Br2 in the visible continuum, J. Chem.Phys., 70(6): 2882.
Nieuwpoor T WC, De-Jong WA, Visscher L (1997). Relativistic and correlated calculations on the ground, excited, and ionized states of iodine, J. Chem. Phys. 107: 9046.
Rakitzis TP, Kitsopoulos TN (2002). Measuring the Cl and Br photofragment alignment using Slice. Imaging, J. Chem. Phys., 116: 9228.
Siegbahn JA, Per EM, Anders H, Bjorn OR (1981). J. Chem. Phys., 74(4): 2384.
Teichteil C, Pelissier M (1994). Relativistic calculations of excited states of molecular iodine, Chem. Phys., 180: 1.